Feasibility Demonstration of Spatial Channel Networking Using SDM/WDM Hierarchical Approach for Peta-b/s Optical Transport

Masahiko Jinno, *Fellow, IEEE, Member, OSA*, Takahiro Kodama, *Member, IEEE*, and Tsubasa Ishikawa

(Highly-Scored Paper)

***Abstract*—This article reports on a proof of concept demonstration of a recently proposed spatial channel network (SCN) that was conducted over an SCN testbed that comprises low-loss hierarchical optical cross-connect (HOXC) prototypes and four-core multicore fiber links. The HOXC prototypes used in the testbed are based on sub-matrix-switches and core selective switches both implemented with commercially available discrete optical switches. Using these two types of HOXC prototypes, the spatial channel networking including spatial bypassing, spatial add/drop and spectral grooming, spatial-lane change, and spatial-channel (SCh) protection is successfully demonstrated for SChs carrying 100-Gb/s–900-Gb/s optical channels.**

***Index Terms*—Core selective switch, matrix switch, spatial bypass, spatial channel, spatial cross-connect, spatial division multiplexing, wavelength division multiplexing.**

GLOSSARY

AC	Any-core access
B&S	Broadcast and select
ClL	Colorless
CnL	Contentionless
CSS	Core selective switch
D	Directional
FC	Fixed-core access
HOXC	Hierarchical optical cross-connect
LC	Lane change
MCF	Multicore fiber
MEMS	Micro electro-mechanical systems
MS	Matrix switch
ND	Non-directional
NLC	Non-lane change
OCh	Optical channel
OH	Overhead information
OMS	Optical multiplexing section
OTN	Optical transport network
R&S	Route and select
ROADM	Reconfigurable optical add drop multiplexer
SCh	Spatial channel
SCN	Spatial channel network
SDEMUX	Spatial demultiplexer
SDM	Space division multiplexing
SL	Spatial lane
SMF	Single mode fiber
SMUX	Spatial multiplexer
SXC	Spatial cross-connect
WDM	Wavelength demultiplexer
WSS	Wavelength selective switch
WXC	Wavelength cross-connect

Manuscript received November 28, 2019; revised January 17, 2020; accepted January 24, 2020. Date of publication February 7, 2020; date of current version May 6, 2020. This work was supported in part by the JSPS KAKENHI under Grant 26220905 and Grant JP18H01443, and the National Institute of Information and Communication Technology (NICT) under Grant 19302 and Grant 20401. *(Corresponding author: Masahiko Jinno.)*

The authors are with the Faculty of Engineering and Design, Kagawa University, Takamatsu 761-0396, Japan (e-mail: jinno@eng.kagawa-u.ac.jp; tkodama@emg.kagawa-u.ac.jp; s16t284@stu.kagawa-u.ac.jp).

Color versions of one or more of the figures in this article are available online at https://ieeexplore.ieee.org.

Digital Object Identifier 10.1109/JLT.2020.2972367

I. INTRODUCTION

THE continuing growth in the amount of Internet traffic keeps fueling an increasing demand for bandwidth in optical networks. A recent report predicted that commercial 10-Tb/s optical interfaces working in 1-Pb/s optical transport systems will be needed by around 2024 [1]. Since a 10-Tb/s dual-polarization (DP) quadrature phase shift keying (QPSK) superchannel occupies at least a 3.2-THz spectrum, conventional single mode fibers (SMFs) can accommodate only a single optical channel (OCh) in the C-band. Certainly, we can employ spectrally efficient higher order modulation formats at the expense of an extremely shorter optical reach; however, we only gain a few additional years before a spectral superchannel will occupy the entire C band. It is quite clear that for such an ultra-high capacity superchannel, the wavelength switching layer is no longer necessary as suggested in [1]. In addition, the foreseeable 1-Pb/s optical transport system capacity in 2024 will far exceed the conventional SMF capacity limit. As a consequence, there will be a need for massive parallel SMFs (for example, a few dozens to approximately 100) and/or newly-developed spatial division multiplexing (SDM) fibers with numbers of spatial modes between adjacent optical nodes. Among the wide variety of SDM fibers reported so far, an uncoupled multicore fiber (MCF) has advantages over other new core-structure fibers such as a multimode fiber or a coupled core MCF, especially for terrestrial networks, because it is compatible with the current SMF-based

transmission technologies in terms of not requiring complicated multiple-input multiple-output digital signal processing for spatial demultiplexing. On the other hand, historically speaking, a new multiplexing technology comes with a new networking layer and a switching technology with the same switching granularity as the multiplexing granularity of the layer. For example, time division multiplexing required synchronous digital hierarchy cross-connects or optical channel data unit cross-connects, and WDM required reconfigurable optical add drop multiplexers (ROADMs) or wavelength cross-connects (WXCs).

According to these observations, it would be natural to introduce spatial channel cross-connects (SXCs) that perform core-level switching to achieve a cost-effective SDM layer. In this scenario, the optical layer should evolve to the hierarchical SDM and WDM layers and an optical node should be decoupled into an SXC and a WXC to form a hierarchical optical cross-connect (HOXC). Based on this idea, we recently proposed a spatial channel network (SCN) architecture that employs a spatial bypass through a potentially low-loss and cost-effective SXC [2], [3]. In an SCN, a spatial channel (SCh) is defined as an ultra-high capacity optical data stream that is allowed to occupy the entire available spectrum of a core in an SMF or an uncoupled MCF. If there is a single or aggregate traffic flow that is sufficiently large to fill almost the entire bandwidth of an SCh between the source and destination nodes, an SCh, which *spatially-bypasses* the overlying WDM layer through SXCs on the route, is established between them. If there is an insufficient amount of traffic between a source/destination pair, the corresponding OCh shares an SCh with other low capacity OChs that have different source/destination pairs by using a WXC for better spatial resource utilization (*spectral grooming*). This results in the cost-effective transport of OChs with a wide variety of bandwidths and an expanded optical reach for spatially bypassed OChs [3]–[5].

As growable and reliable SXC architectures, we proposed two modular SXC architectures. One is based on a sub-matrix-switch (sub-MS) and the other is based on a core selective switch (CSS) [2], [3]. The former is a moderate-sized single stage MS and the latter is a novel optical spatial switch that is the SDM counterpart of a wavelength selective switch (WSS) in a WDM network. By choosing working and backup routes so that they are SDM link disjoint and sub-MS (CSS) disjoint from each other, the proposed two SXC architecture supports fault-independent *SCh protection*, which covers both an SDM link failure and a sub-MS (CSS) failure. The SCh protection is advantageous over the OCh protection in terms of an SDM link failure because a much smaller number of channels needs to be rerouted resulting in much quicker recovery from an SDM link failure.

We recently constructed an SCN testbed and conducted spatial channel networking experiments employing the proposed two types of HOXC prototypes, each based on sub-MSs and CSSs respectively, for the first time [6]. The HOXC prototypes were built using commercially available discrete optical switches. The aim of the experiments is to demonstrate the feasibility of SCN networking in terms of the *spatial bypass* via an SXC, the *spatial add/drop and spectral grooming* in an HOXC, and the *SCh protection*. Although numerous discrete $1 \times$ N optical switches were required to implement the CSSs in this principle demonstration experiment, we expect to achieve much simpler and cost-effective CSSs by employing free-space optics as we recently reported in [7] and [8].

This paper is an expanded version of [6]. The remaining part of this paper is structured as follows. In Section II, we describe related work in terms of optical network architectures and optical node architectures. In Section III, we briefly describe the SCN architectures and networking functionalities to be verified. In Section IV, we explain the SCN testbed. In Section V, we show two types of SXC architectures based on a sub-MS and a CSS and their prototypes that are implemented using commercially available spatial switches. In Section VI, we describe the experimental configuration for a feasibility demonstration of spatial channel networking including using 100-Gb/s to 900-Gb/s spectral superchannels and present the experimental results. In Section VII, we summarize our conclusions.

II. Related Work

Since we expect to reach the fundamental capacity limits of conventional SMFs, research over the past 10 years has focused on SDM as the only remaining signal multiplexing technology [1]. A near-term solution is to use existing parallel SMFs and a middle term solution would be to introduce uncoupled MCFs. Although SDM technology significantly scales in spatial mode counts, S, per link and network capacity, it presents a challenge in that it necessitates the deployment of large ROADMs comprising a large number ($= 2DS$) of high port count ($\geq DS$) WSSs where D is the node degree [3]. In order to deal with this problem, research has been dedicated to developing scalable WDM/SDM ROADM architectures supporting a large number of SMFs or SDM fibers [9]–[19]. One such approach is to operate a high port count WSS in a *joint switching* mode [9]–[14]. A joint-switching ROADM jointly switches spatial superchannels, which are high-rate data streams transported as groups of subchannels occupying the same frequency slot in separate modes/cores of an SDM fiber. Spectrally and spatially flexible optical networking architectures that support the joint switching of spatial superchannels were discussed in [15] and [16]. Sato *et al.* took another approach. Instead of creating a high-port count ROADM using a large number of cascaded conventional WSSs or ultra-high port count WSSs, they introduced a subsystem-modular WXC architecture in which multiple small-scale WXC subsystems (sub-WXCs) are connected via a limited number of intra-node SMFs. The total WXC port count can be simply expanded by adding sub-WXCs [17]–[19].

It should be noted that although the joint-switching ROADMs and subsystem-modular WXCs can support SDM fibers, they are designed for use in single-layer WDM networks [3]. This means that so long as they handle traffic demands only in the fine granular WDM layer, they will most likely be less cost-effective in the forthcoming massive SDM era. For example, a joint switching ROADM that supports S spatial modes per link requires high-port count WSSs with S times the port count of that of a conventional WSS. A subsystem-modular WXC that supports S spatial modes per link requires a large number of conventional WSSs, which is S times the number of that needed in a conventional WXC.

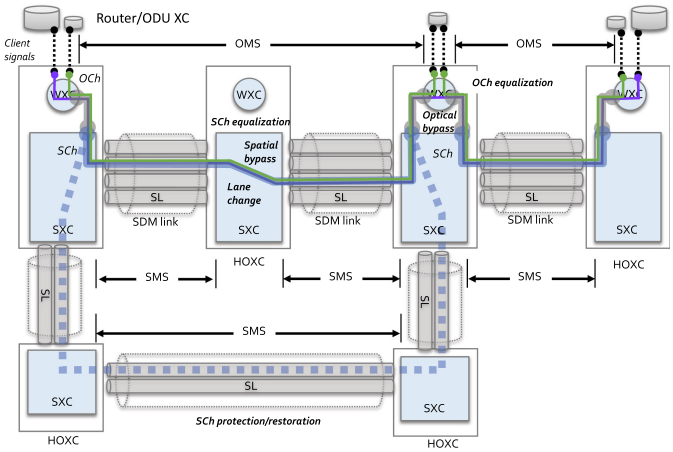

Fig. 1. SCN architecture and functionalities.

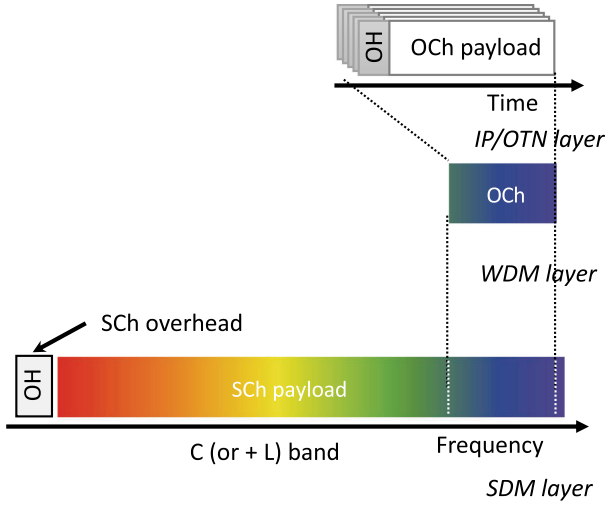

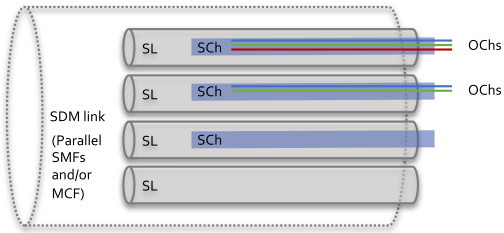

Fig. 2. Nested structure of OCh, SCh, SL, and SDM link.

Our approach, SCN, is totally different to the above described single layer approaches [3]. In an SCN, the optical layer is explicitly divided into the WDM layer and the SDM layer to form a hierarchical optical network, and an optical node is decoupled into an SXC and a WXC to form an HOXC. As a matter of fact, the idea of hierarchical (or multi-granular) optical networks, in which coarser granular but more cost-effective switching layer(s) than the wavelength layer is introduced, is not new at all. The concepts of coarser granular optical switching in the wavelength-band and fiber layers were already proposed at the end of the '90s [20]–[22]. Since then, there have been considerable research efforts [23], [24]; however, they have remained rather marginal even after SDM technology began to gather much attention [25]–[27]. Furthermore, to the best of our knowledge, there are no reports that have focused on practical issues such as the growability, reliability, and techno-economics of hierarchical optical node architectures before we proposed the SCN concept and enabling SXC architectures [3].

III. SCN Architecture and Networking Functionalities

A. SCN Architecture

Fig. 1 shows the architecture of an SCN that comprises HOXCs and SDM links. An HOXC comprises an SXC and a WXC. An SDM link is assumed to comprise parallel SMFs or an uncoupled MCF. Although the SCN concept could be expanded to support other SDM fibers such as a few-mode fiber, a coupled core fiber, and a few-mode multi-core fiber, we leave this for future study. Here, we refer to a spatial resource unit in an SDM link as a spatial lane (SL), whose physical entity is a core in parallel SMFs or an MCF. In an SDM link, each SL may be labeled with its identification number. We define the section between adjacent SXCs as a spatial multiplexing section (SMS). The SMS is similar to an optical multiplexing section (OMS) in an optical transport network (OTN), which is defined as a section between adjacent WXCs. An OMS may traverse contiguous multiple SMSs. Clearly, an optical amplification function is indispensable in order to compensate for the transmission loss of an SDM link and the insertion loss of an SXC, but it is not depicted in Fig. 1 for simplicity. If SDM links comprise parallel SMFs, optical amplification is achieved by using an array of conventional erbium-doped fiber amplifiers (EDFAs). If SDM links comprise MCFs, optical amplification is achieved by using an EDFA with an MCF input/output, which may be, for example, a cladding pumping MCF EDFA [28] or may comprise a micro SMF EDFA array [29].

In an SCN, we introduce the concept of a SCh. An SCh is defined as an ultra-high capacity optical data stream that is allowed to occupy the entire available spectrum of an SL. An SCh may include an in-band overhead channel (SCh OH) that carries operations, administration, and maintenance information such as a path trace and maybe some kind of performance monitoring information. It is spatially routed and amplified end to end along with an SCh payload through SXCs bypassing the overlying WDM layer. Optical (wavelength) channels each having a wide variety of spectral widths arranged on the flexible grid are accommodated in an SCh. The nested structure of an OCh, SCh, SL, and SDM link in an SCN is shown in Fig. 2. Just as an OCh provides a virtual topology between routers or optical transport data unit (ODU) cross-connects (XCs), an SCh may provide a virtual topology between WXCs.

B. SCN Networking Functionalities and Their Benefits

1) Spatial Bypass: An SCh is established if there is a single or aggregate traffic flow that is sufficiently large to fill almost the entire bandwidth of an SCh between the source and destination nodes. Such SChs bypass the overlying WDM layer (*spatial*

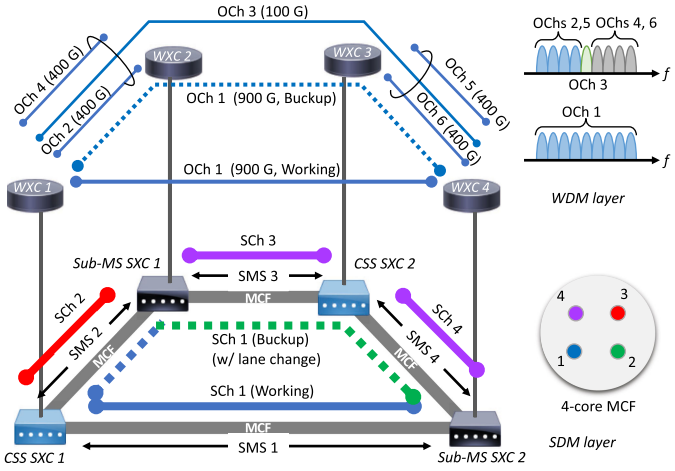

Fig. 3. Logical configuration of SCN testbed.

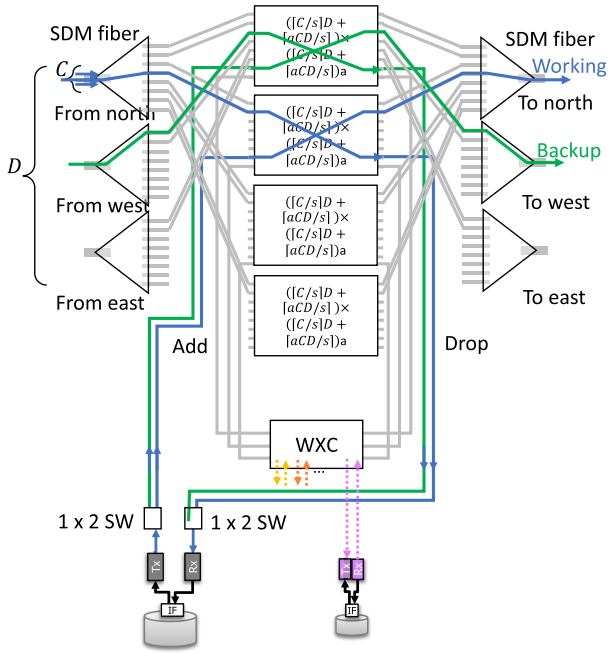

Fig. 4. HOXC architecture based on single-stage sub-MSs.

bypass). Thanks to the low-cost coarse granular switching and low-insertion loss characteristics of SXCs, they enjoy a lower switching cost per bit and an extended optical reach.

2) Spatial Add/Drop and Spectral Grooming: If there is an insufficient amount of traffic between a source/destination pair, the corresponding OCh shares an SCh with other low capacity OChs having different source/destination pairs for better spatial resource utilization. SChs carrying such low capacity OChs, which are either destined for the site (*optical drop*) or being further groomed (*optical bypass*) in the WDM layer by a WXC at the site, are dropped by the SXC (*spatial drop*). The latter OChs are described as "spectrally groomed." This enables us to deploy only the necessary minimum number of fine granular WXCs in an SCN.

3) SL Change: Even when there is no common unused SL index for each SDM link on the route, an SCh could be established if an SXC on the route has the ability to change SLs. This means that the SL change capability allows us to assign SLs independently to each link. Lane change (LC) in the spatial domain, which can be performed using an MS, is easier to implement than LC in the wavelength domain, which is referred to as wavelength conversion and requires expensive optical-to-electrical-to-optical conversion. Introducing an SXC may be an opportunity to enhance the degree of connectivity freedom in the optical domain.

4) SCh Protection/Restoration: If there is a fiber cut or an SXC failure on the route for an SCh, SXCs located at the end points of the SCh may switch over the routes from the original route to the pre-planned detour route (SCh protection) or a network management system may collect surviving network resource information, calculate detour routes, and reconfigure the SDM layer through control of SXCs (SCh restoration).

IV. Spatial Channel Network Testbed

In order to verify the feasibility of the SCN networking functionalities described in the previous section, we constructed an SCN testbed. The logical configuration of the testbed is shown in Fig. 3, which is a ring network that comprises four SXCs, two are sub-MS-based SXCs (sub-MS SXCs) and the other two are CSS-based SXCs (CSS SXCs). Spatial multiplexing sections, SMS 1, SMS 2, SMS 3, and SMS 4, are defined between adjacent SXCs. Different types of SXCs are connected alternately via a 4-core MCF. Each SXC is connected to a WXC via conventional SMFs. SChs and OChs shown in Fig. 3 are established over the testbed to demonstrate the SCN networking functionalities described below. The color of each SCh corresponds to an SL in a four-core MCF through which the SCh traverses.

- *Spatial bypass:* A high-bit-rate 900-Gb/s spectral superchannel (OCh 1) is accommodated in a working SCh (SCh 1(w)) and its link-disjoint backup (SCh 1(b)). They are express SChs and spatially bypass overlying WXCs.
- *Spatial add/drop and spectral grooming:* Low capacity OChs with different endpoints may be bundled into the same SCh and groomed at a WXC to form well-packed SChs. A 100-Gb/s OCh (OCh 3) is carried through SCh 2, SCh 3, and SCh 4 while being bundled with a 400-Gb/s spectral superchannel (OCh 2, OCh 4, OCh 5, and OCh 6) and groomed in the WDM layer.
- *SL change:* SCh 1(b) changes SLs at sub-MS-SXC 2 from SL 1 to SL 2.
- *SCh protection:* When link failure occurs at SMS 1, spatial switches at the endpoints of SCh 1(w) are activated to switch over SCh 1(w) to SCh 1(b).

V. HOXC Architectures and Prototypes

A. HOXC Architectures Employed in SCN Testbed

1) Sub-MS-Based SXC Architecture: Fig. 4 shows an HOXC architecture based on single-stage $(C/sD + aCD/s\,) \times (C/sD + aCD/s)$ sub-MSs, where C is the number of single-mode cores per link, D is the node degree, a is the add

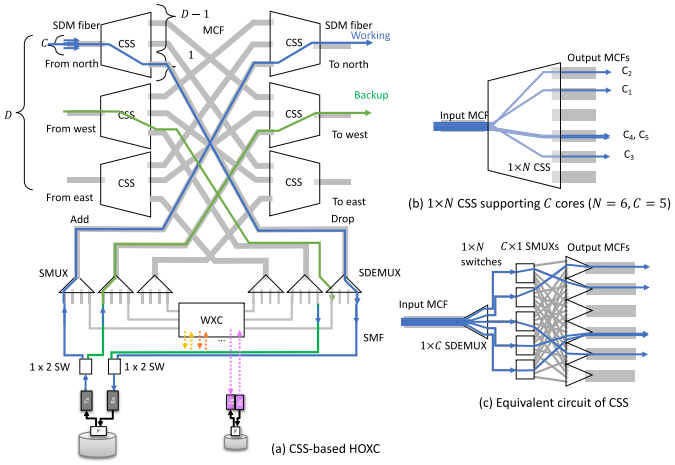

Fig. 5. HOXC architecture based on CSSs.

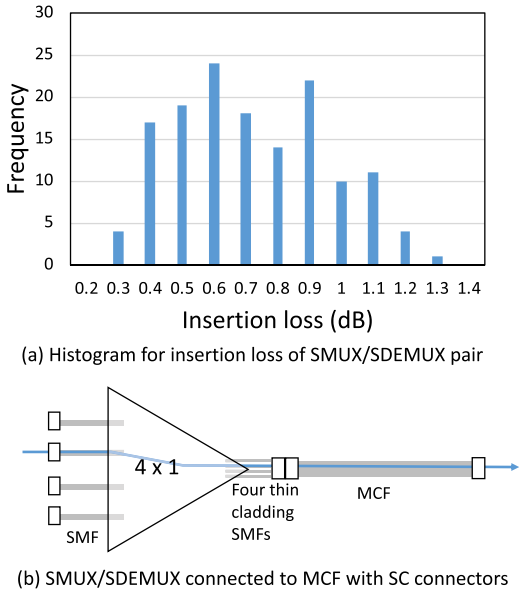

Fig. 6. IL characteristics of employed SMUX/SDEMUX.

drop ratio of the SXC, and s is the partitioning number of cores. Here, $D\ (=3)$ ingress (egress) MCFs from (to) different directions that support $C\ (=8)$ cores are connected on the ingress (egress) side of the SXC via $1 \times C$ spatial demultiplexers (SDEMUXs) ($C \times 1$ spatial multiplexers (SMUXs)). Eight cores in an MCF are partitioned into $s\ (=4)$ core groups, each comprising $C/s\ (=2)$ cores, and each core group in an MCF is accommodated in a different sub-MS. If the add drop ratio for SXC a of $1/3$, is assumed, a sub-MS should have $C/sD + aCD/s(=8)$ input (output) ports for through traffic and add (drop) traffic. In this architecture, a core that belongs to a core group can only be connected to a core in a different direction or a transceiver that belongs to the same core group. Instead, this architecture achieves growability in terms of SLs and supports fault independent protection by choosing working and backup routes so that they are SDM link disjoint and sub-MS disjoint [2], [3]. Hereafter, we refer to these features (constraints) of the sub-MS based SXC as *partial any-core access* (partial AC), *non-directional* (ND), contention-less (CnL), and *partial lane change* (partial LC), respectively. Regarding a WXC overlying the SXC, each port of the WXC is connected to a different sub-MS in order to prepare for the event of a sub-MS failure.

2) CSS-Based SXC Architecture: Fig. 5(a) shows the HOXC architecture based on a $1 \times D\ (=3)$ CSS supporting $C(=4)$ cores with a $1 \times C$ SDEMUX/SMUX at a local port. Here, a CSS is the SDM counter part of a WSS in the current WDM network, which has an input MCF and N output MCFs where each MCF has C cores in its cladding as shown in Fig. 5(b) ($N = 6$, $C = 5$ in the figure). Its equivalent circuit can be expressed as shown in Fig. 5(c). Optical signals propagated through cores of the input MCF are spatially demultiplexed by a $1 \times C$ SDEMUX and launched into $1 \times N$ switches. Each optical signal is then routed and spatially multiplexed with a $C \times 1$ SMUX into its output MCFs.

In Fig. 5(a), ingress and egress CSSs linked to MCF transmission lines are arranged in the *route and select* (R&S) configuration instead of the simpler *broadcast and select* (B&S) configuration. This is to avoid the inherent splitting loss of an optical splitter used in the B&S configuration and to achieve a low insertion loss SXC that actualizes an optical reach for a spectrally groomed OCh in an SCN that is almost the same as the optical reach in a current WDM network as described in the previous sub-section. Among D output ports of the CSS, $D-1$ ports are for through SChs and the remaining port that is linked to an SDEMUX (SMUX) is for local drop (add) SChs.

In this architecture, an unused input port on an SMUX can be connected to an unused core with the index associated to the SMUX input port on the egress MCF to which the SMUX is linked. This architecture does not provide a LC capability. Hereafter, we refer to these features (constraints) of the CSS based SXC as *fixed core access* (FC), ND, CnL, and *non-lane change* (NLC), respectively. Clearly, there must be a wide variety of add/drop part architectures and technologies to achieve more flexible connectivity. Detailed discussion can be found in [30].

B. Building Blocks

MCFs used in the testbed have standard 125-μm cladding and support four single mode cores arranged with a 45-μm core spacing [31]. The SDEMUX/SMUX used in the SCN testbed is a SMF bundle type, in which four thin-cladding SMFs are bundled in a standard connector ferrule for an SMF to form an interface to an MCF connector [32]. Fig. 6(a) shows a histogram of the insertion loss (IL) of an SMF-bundle type SMUX including the connection loss to an MCF code for all the combinations of six SMUXs and six MCF codes that we have in our laboratory, which are measured in the configuration shown in Fig. 6(b). The average and worst ILs for the SMUXs including the connection loss to an MCF are 0.7 dB and 1.2 dB, respectively. The two 16×16 sub-MSs used in the testbed are achieved by dividing a commercial 32×32 MS. Fig. 7(a) shows a histogram of the ILs among all the combinations of input and output ports of the 16×16 MS shown in Fig. 7(b). The average and worst ILs of

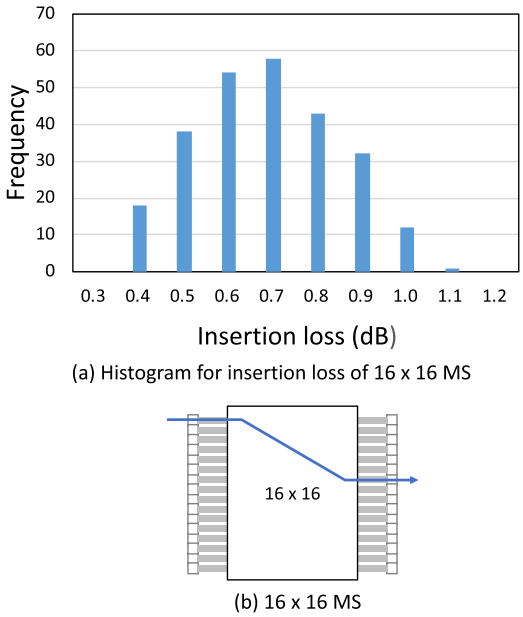

Fig. 7. IL characteristics of employed MS.

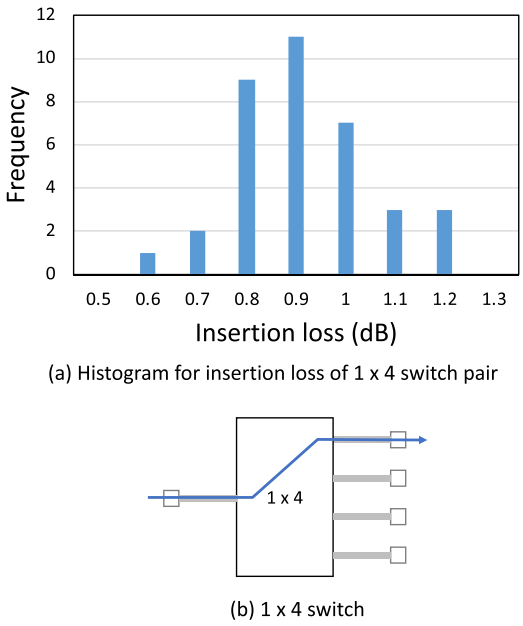

Fig. 8. IL characteristics of employed 1×4 SW.

the sub-MS are 0.7 dB and 1.1 dB, respectively. Fig. 8(a) shows a histogram of the IL between the input and four output ports of the nine 1×4 spatial switches shown in Fig. 8(b). The average and worst ILs of 1×4 spatial switches are 0.9 dB and 1.1 dB, respectively.

C. Requirement for SXC IL

As described in [3] and [4], a requirement for practical SXCs from the viewpoint of physical performance is that the SXC

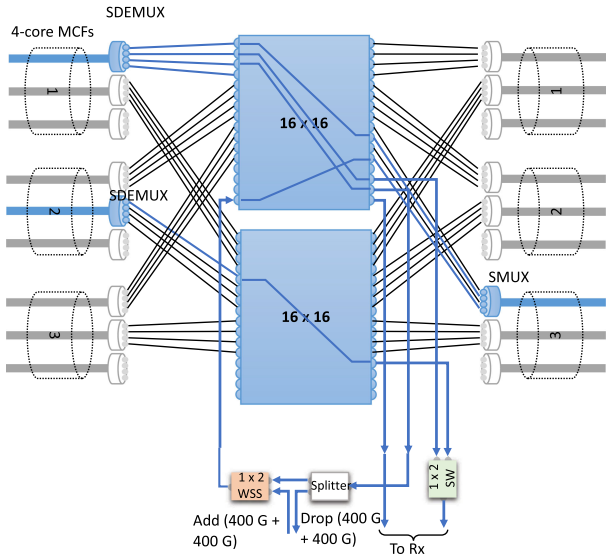

Fig. 9. Sub-MS based HOXC prototype.

insertion loss must be sufficiently low to deter degradation in the transmission performance of OChs that are spectrally groomed by a WXC. Gaussian noise model [33], [34] analysis revealed that if we assume, for example, a 20-dB transmission loss per link (corresponding to a 80-km fiber span when the fiber loss is 0.25 dB/km) and a 20-dB insertion loss per WXC (a typical loss value for a WXC employing the B&S architecture equipped with some performance monitoring points), in order to achieve a optical reach that is at almost the same level as that for an OCh transported through a conventional single-layer WDM network (for example $> 95\%$), we will need an SXC with an insertion loss of less than 7 dB [3], [4].

D. HOXC Prototypes

1) Sub-MS-Based HOXC Prototype: Fig. 9 shows a sub-MS based HOXC prototype used in the SCN testbed. We assumed that each SDM link comprises three four-core MCFs, but only the MCFs indicated in blue are implemented due to the limited availability of equipment. We use two 16×16 MSs that are sandwiched between a 1×4 SDEMUX and 4×1 SMUX to achieve a sub-MS SXC that supports three four-core MCFs per link, three nodal degrees, and an add/drop ratio of $1/3$. The connections indicated in black in Fig. 9 are not implemented. According to the IL measurement results for the SMUXs and MSs as described in the previous subsection, we expect that the ingress MCF to the egress MCF loss of the SXC based on sub-MSs is 2.3 dB on average and 3.7 dB for the worst case. This is much lower than the maximum allowable insertion loss of 7 dB for an SXC as explained in the previous sub-section.

A simple 1×2 switch is used for SCh protection. A WXC that comprises a 3-dB splitter and a 1×2 conventional WSS is connected to add/drop ports of the sub-MS. This SXC prototype is SL changeable among four SLs and is resilient against both fiber and switch failures because it accommodates working and backup SChs in different sub-MSs.

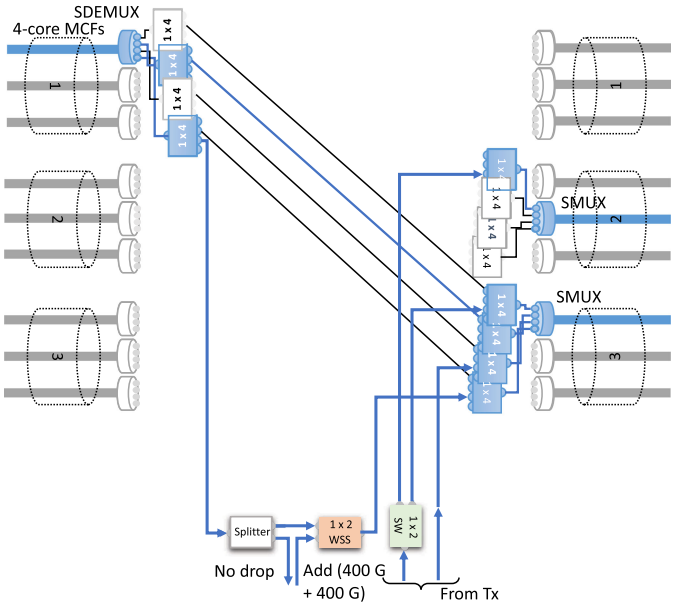

Fig. 10. CSS based HOXC prototype.

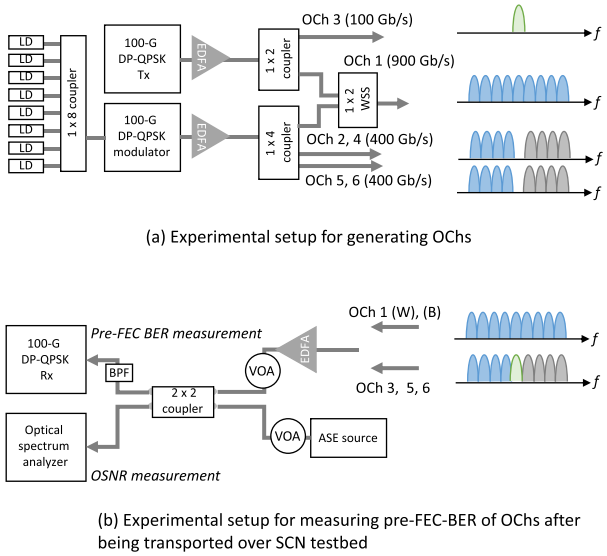

Fig. 11. Experimental configuration for generating and measuring OChs.

2) CSS-Based HOXC Prototype: There are currently no commercially-available CSSs. One possible approach to achieve a CSS is to combine discrete devices such as an SDEMUX device, an array of $1 \times N$ spatial switches, and N SMUX devices to form a CSS equivalent circuit as shown in Fig. 5(c). Another possible approach is to employ free space optics [7], [8], which is an approach similar to that for current commercial WSSs but has a rather simpler multiplexing/demultiplexing part. We employed, in this principle demonstration, a commercial 1×4 spatial switch array that is arranged to form an R&S configuration as shown in Fig. 10. We assumed that each SDM link comprises three four-core MCFs, but only the MCFs indicated in blue were implemented due to the limited availability of equipment. In addition, we did not implement output SMUXs in the CSSs, instead we used parallel SMFs to connect input and output CSSs because the available number of SMUX/SDEMUX devices were limited. Since this CSS-SXC architecture is port-modular, it supports fault-independent SCh protection by choosing working and backup routes to be SDM-link-disjoint from each other. According to the IL measurement results of the SMUXs and 1×4 spatial switches as described in the previous subsection, we expect that the ingress MCF to egress MCF loss of the SXC based on CSSs is 3.4 dB on average and 5.0 dB in the worst case. This is also lower than the maximum allowable insertion loss of 7 dB for an SXC.

VI. SCN Networking Demonstrations

Fig. 11(a) shows the experimental configuration to generate each spectral superchannel used in the testbed. A 100-Gb/s dual-polarization QPSK transmitter is employed to generate an optical (sub-)channel under pre-forward error correction (FEC) bit-error-rate (BER) measurement. Eight wavelength-tunable laser diodes and a 100-Gb/s dual-polarization QPSK modulator are employed to generate other optical sub-channels. By copying and multiplexing these optical signals using optical splitters and a 1×2 WSS, a 900-Gb/s superchannel (OCh 1), 400-Gb/s superchannels (OCh 2, OCh 4, OCh 5, and OCh 6), and a 100-Gb/s channel (OCh 3) are created.

Due to the limited availability of optical switches and SMUXs/SDEMUXs, we emulated the four-HOXC ring network shown in Fig. 3 using a figure-eight double-loop network configuration comprising two HOXCs, one is based on a sub-MS and the other is based on a CSS as shown in Fig. 12. This emulation is achieved by transforming the original four-node ring network linked by four MCFs (Fig. 12(a)) to the two-node figure-eight double-loop network linked by three MCFs (Fig. 12(b)) and letting OCh 1 (900 Gb/s) carried by SCh 1 (backup) and OCh 3 (100 Gb/s) carried by SCh 2, SCh 3, and SCh 4 in Fig. 3 traverse the sub-MS based SXC and the CSS-based SXC twice. Fig. 12(c) illustrates the actual experimental network configuration. The two boxes labeled "Sub-MS-SXCs 1, 2" and "CSS-SXCs 1, 2" are the SXC prototypes described above.

Fig. 13 shows states of the SL assignment in the four-core MCFs at SMS 1, SMS 2, and SMS 3 for the normal state and rerouting state (in the case of a link failure at SMS 1) as well as spectra for SCh 1, SCh 2, SCh 3, and SCh 4 indicated in an unfolded equivalent network configuration of the SCN testbed shown in Fig. 12(c). States of the SL assignment are shown as images of beams emitted from an MCF connector facet captured by using a spatial beam profiler (SBP). For reference, an image captured by the SBP when all cores are illuminated and a photo of the cross-section of the four-core MCF used in the SCN testbed are shown at the leftmost of Fig. 13.

We confirmed by comparing SBP images for SMS 1, SMS 2, and SMS 4 for the normal state and rerouting state that when a link failure at SMS 1 occurs, SCh 1 (working) carrying 900-Gb/s OCh 1 is successfully switched over to SCh 1 (backup), which spatially bypasses the overlying WXC while changing SLs from SL 1 to SL 2. On the other hand, we see that SCh 2 traversing SL 3, which carries OCh 2, OCh 3, and OCh 4 is dropped at Sub-MS

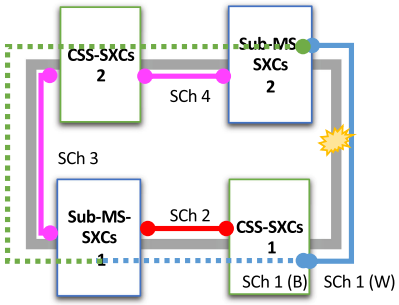

(a) Four-node ring network configuration in the SDM layer

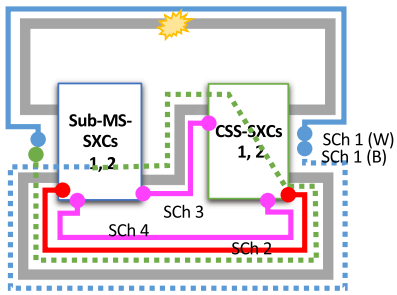

(b) Figure-eight, double-loop network configuration comprising two nodes to emulate the ring network shown in (a)

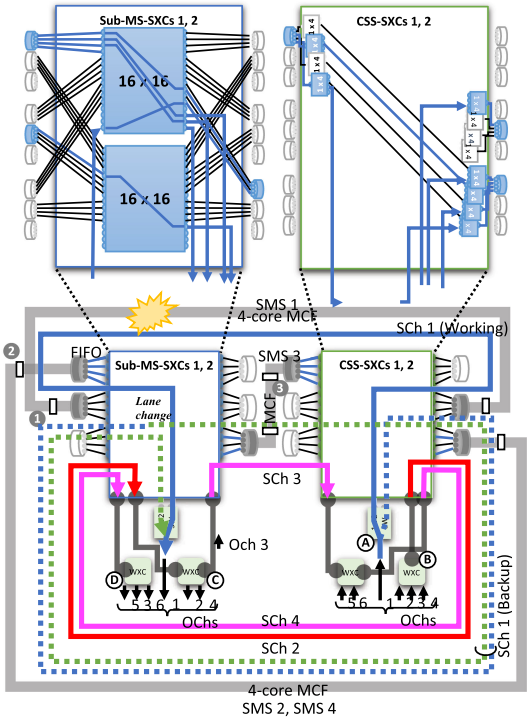

(c) Actual experimental network configuration comprising two HOXC prototypes based on sub-MS and CSS, respectively

Fig. 12. Figure-eight double-loop network configuration comprising a sub-MS based SXC and CSS-based SXC l to emulate four-node ring network.

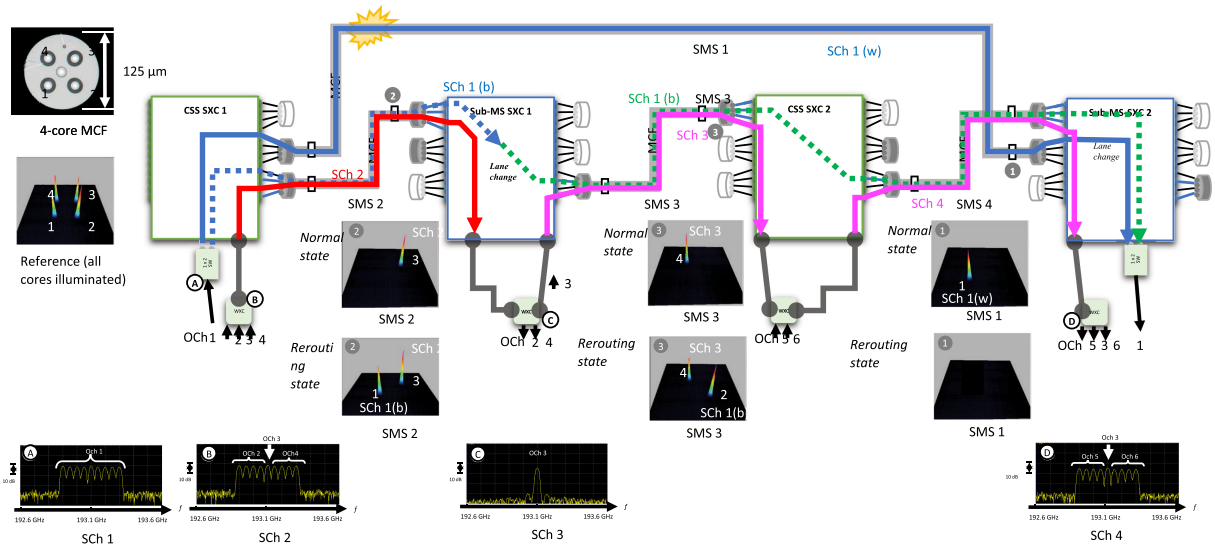

Fig. 13. States of SL assignment in MCFs at SMS 1, SMS 2, and SMS 3 with spectra of SCh 1, SCh 2, SCh 3, and SCh 4.

SXC 1 and only OCh 3 in SCh 2 passes through at WXC 2 and is packed again into SCh 3 that traverses SL 4.

In order to confirm the nonexistence of unknown deteriorating factors in the SCN testbed, we measured the real-time pre-FEC BER performance of the OChs after being transported over the SCN testbed using the experimental configuration shown in Fig. 11(b). The OCh under test is launched into a 100-Gb/s DP-QPSK transmitter together with an amplified spontaneous emission (ASE) light. The pre-FEC BER is measured as the power spectrum density of the ASE light is changed using a variable optical attenuator. Fig. 14 shows the pre-FEC BER versus the OSNR curves for the center subcarrier in OCh 1 carried by SCh 1 (working), the center subcarrier in OCh 1 carried by SCh 1 (backup), and OCh 3 carried by SCh 2, SCh 3, and SCh 4. The back-to-back performance for the employed 100-Gb/s dual-polarization QPSK transmitter is also plotted in

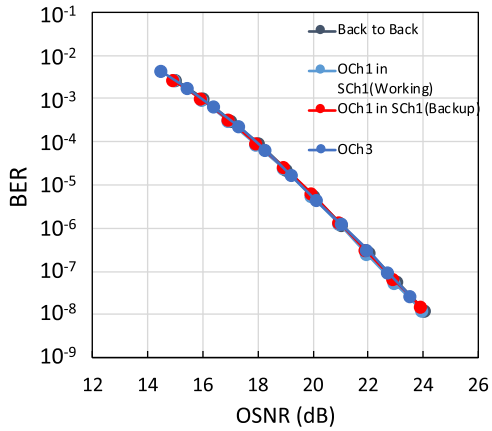

Fig. 14. Pre-FEC BER versus OSNR performance in spatial channel networking experiments.

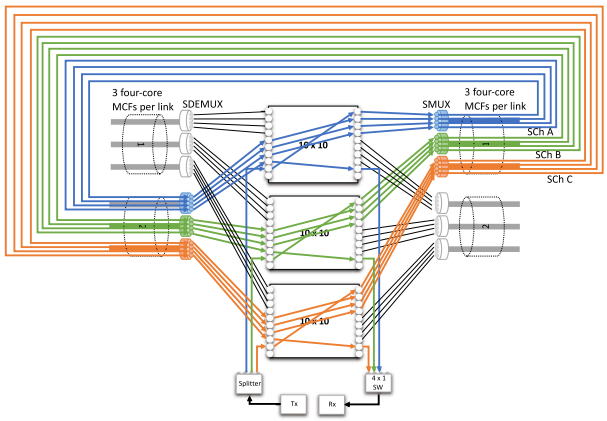

Fig. 15. Recirculating experiment configuration for cascaded sub-MS SXCs.

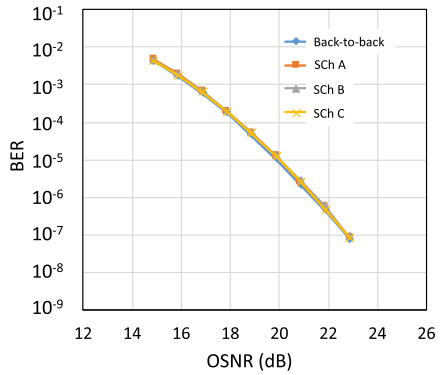

Fig. 16. Pre-FEC BER versus OSNR performance in recirculating experiments.

Fig. 14. The figure shows that no OSNR penalty occurs from the back-to-back performance generated by traversing the SCN testbed. We also conducted a recirculating experiment using the experimental setup shown in Fig. 15 to emulate cascaded sub-MS SXCs where all 12 SLs in an SDM link are fully utilized. We confirmed that no OSNR penalty is generated even after 5 times of routing with sub-MSs and 8 times of multiplexing/demultiplexing with SMUX/SDEMUX devices as shown in Fig. 16.

VII. Conclusions

We conducted a proof of concept demonstration of a recently proposed SCN utilizing an SCN testbed that comprises low-loss HOXC prototypes and four-core MCF links. The HOXC prototypes used in the SCN testbed were based on sub-MSs and CSSs both implemented with commercially available discrete optical switches. The SCh networking including spatial bypassing, spatial add/drop and spectral grooming, spatial-LC, and SCh protection is successfully demonstrated for SCHs carrying 100-Gb/s to 900-Gb/s OChs. Pre-FEC BER measurements for OChs that traversed the SCN testbed confirmed there exists no performance degradation through the SCh networking.

Two SXC architectures tested in the SCN networking testbed have their advantages and disadvantages. At this moment, there is no clear answer to the question of which SXC architecture will achieve techno-economical validity in future SCNs. This is because it depends on many factors such as traffic patterns (dynamic or incremental), fiber types (parallel SMFs or MCF), and the maturity of support technologies (optical amplifiers, optical switches, SMUX/DEMUX, etc.) in future SCNs. We recently analyzed a wide variety of SXC architectures including traditional architectures and the two novel architectures described in this paper from the viewpoints of the freedom of connection functionalities, operational benefits, and potential node costs associated with the architectural complexity [30]. The results may be useful to obtain insights regarding which SXC architecture is suited to a given specific network scenario.

Acknowledgment

The authors thank Furukawa Electric Co., Ltd. for providing the four-core MCFs and 1×4 SMUX/SDEMUX devices.

References

[1] P. J Winzer and D. T Neilson, "From scaling disparities to integrated parallelism: A decathlon for a decade," *J. Lightw. Technol.*, vol. 35, no. 5, pp. 1099–1115, Mar. 2017.

[2] M. Jinno, "Spatial channel network (SCN) architecture employing growable and reliable spatial channel cross-connects toward massive SDM era," in *Proc. Int. Conf. Photon. Switching Comput.*, Sep. 2018, Paper Fr3C.5.

[3] M. Jinno, "Spatial channel network (SCN): Opportunities and challenges of introducing spatial bypass toward massive SDM era [Invited]," *IEEE/OSA J. Opt. Commun. Netw.*, vol. 11, no. 3, pp. 1–14, Mar. 2019.

[4] M. Jinno, "Added value of introducing spatial bypass into WDM/SDM networks: Gaussian-noise model analysis for spatially-bypassed and spectrally-groomed optical channels," in *Proc. Eur. Conf. Opt. Commun.*, 2018, Paper We3D.6.

[5] M. Jinno and Y. Asano, "Required link and node resource comparison in spatial channel networks (SCNs) employing modular spatial channel cross-connects (SXCs)," in *Proc. Opt. Fiber Commun. Conf.*, 2019, Paper M1A.1.

[6] M. Jinno *et al.*, "Demonstration of spatial channel networking using two types of hierarchical optical cross-connects," in *Proc. Eur. Conf. Opt. Commun.*, 2019, Paper Th.1.A.6.

[7] M. Jinno, K. Yamashita, and Y. Asano, "Architecture and feasibility demonstration of core selective switch (CSS) for spatial channel network (SCN)," in *Proc. 24th OptoElectron. Commun. Conf./Int. Conf. Photon. Switching Comput.*, 2019, Paper WA2-3.

[8] M. Jinno, T. Kodama, and T. Ishikawa, "Five-core 1 × 6 core selective switch and its application to spatial channel networking," in *Proc. Opt. Fiber Commun. Conf. Exhib.*, 2020, Paper M3F.2.

[9] D. M. Marom and M. Blau, "Switching solutions for WDM- SDM optical networks," *IEEE Commun. Mag.*, vol. 53, no. 2, pp. 60–68, Feb. 2015.

[10] M. D. Feuer *et al.*, "ROADM system for space division multiplexing with spatial superchannels," in *Proc. Optical Fiber Commun. Conf. Exhib.*, 2013, Paper PDP5B.8.
[11] L. E. Nelson *et al.*, "Spatial superchannel routing in a two-span ROADM system for space division multiplexing," *J. Lightw. Technol.*, vol. 32, no. 4, pp. 783–789, Feb. 2014.
[12] N. K. Fontaine *et al.*, "Heterogeneous space-division multiplexing and joint wave- length switching demonstration," in *Proc. Optical Fiber Commun. Conf. Exhib.*, 2015, Paper Th5C.5.
[13] M. Jinno and Y. Mori, "Unified architecture of an integrated SDM-WSS employing a PLC-based spatial beam transformer array for various types of SDM fibers," *J. Opt. Commun. Netw.*, vol. 9, no. 2, pp. A198–A206, 2017.
[14] Y. Mori, K. Yamashita, and M. Jinno, "Feasibility demonstration of integrated fractional joint switching WSS applicable for few-mode multicore fiber," in *Proc. Photon. Switching Comput.*, 2018, Paper Fr3C.3.
[15] D. Klonidis *et al.*, "Spectrally and spatially flexible optical network planning and operations," *IEEE Commun. Mag.*, vol. 53, no. 2, pp. 69–78, Feb. 2015.
[16] R. Proietti *et al.*, "3D elastic optical networking in the temporal, spectral, and spatial domains," *IEEE Commun. Mag.*, vol. 53, no. 2, pp. 79–87, Feb. 2015.
[17] Y. Iwai, H. Hasegawa, and K. Sato, "A large-scale photonic node architecture that utilizes interconnected OXC subsystems," *Opt. Express*, vol. 21, no. 1, pp. 478–487, 2013.
[18] M. Niwa, Y. Mori, H. Hasegawa, and K. Sato, "Tipping point for the future scalable OXC: What size M × M WSS is needed?" *J. Opt. Commun. Netw.*, vol. no. 9, pp. A18–A25, 2017.
[19] R. Hashimoto *et al.*, "First demonstration of subsystem-modular optical cross-connect using single-module 6 × 6 wavelength-selective switch," *J. Lightw. Technol.*, vol. 36, no. 7, pp. 1435–1442, Apr. 2018.
[20] K. Harada, K. Shimizu, and T. Kudou, "Hierarchical optical path cross-connect systems for large scale WDM networks," in *Proc. Tech. Digest. Opt. Fiber Commun. Conf./Int. Conf. Integr. Opt. Opt. Fiber Commun.*, 1999, vol. 2, pp. 356–358.
[21] M. Jinno, J. Kani, and K. Oguchi, "Ultra-wide-band WDM networks and supporting technologies," in *Proc. NOC' 99, Core Netw. Manage.*, 1999, pp. 90–97.
[22] A. A. M. Saleh and J. M. Simmons, "Architectural principles of optical regional and metropolitan access networks," *J. Lightw. Technol.*, vol. 17, no. 12, pp. 2431–2448, Dec. 1999.
[23] X. Cao, V. Anand, and C. Qiao, "Framework for waveband switching in multigranular optical networks: I-multigranular cross-connect architectures," *J. Opt. Netw.*, vol. 5, no. 12, pp. 1043–1055, 2006.
[24] K. Ishii, H. Hasegawa, K. Sato, M. Okuno, S. Kamei, and H. Takahashi, "An ultra-compact waveband cross-connect switch module to create cost-effective multi-degree reconfigurable optical node," in *Proc. Eur. Conf. Exh. Opt. Commun.*, 2009, Paper 4.2.2.
[25] M. Cvijetic, I. B. Djordjevic, and N. Cvijetic, "Dynamic multidimensional optical networking based on spatial and spectral processing," *Opt. Express*, vol. 20, no. 8, pp. 9144–9150, 2012.
[26] N. Amaya *et al.*, "Fully-elastic multi-granular network with space/frequency/time switching using multi-core fibres and programmable optical nodes," *Opt. Express*, vol. 21, no. 7, pp. 8865–8872, 2013.
[27] G. M. Saridis *et al.*, "Experimental demonstration of a flexible filterless and bidirectional SDM optical metro/inter-DC network," in *Proc. Eur. Conf. Opt. Commun.*, 2016, Paper M.1.F.3.
[28] Y. Jung, S, Jain, S. Alam, and D. J. Richardson, "Fully integrated SDM amplifiers," *Proc. 23rd Opto-Electron. Commun. Conf.*, 2018, Paper 4C2-1.
[29] T. M. Paskov *et al.*, "Demonstration of potential 130.8 Tb/s capacity in power-efficient SDM transmission over 12,700 km using hybrid micro-assembly-based amplifier platform," in *Proc. Opt. Fiber Commun. Conf. Exhib.*, 2019, Paper M2I.4.
[30] M. Jinno, "Spatial channel cross-connect architectures for spatial channel networks," *IEEE J. Sel. Topics Quantum Electron.*, to be published.
[31] T. Gonda, K. Imamura, R. Sugizaki, Y. Kawaguchi, and T. Tsuritani, "125 μm 5-core fibre with heterogeneous design suitable for migration from single-core system to multi-core system," in *Proc. Eur. Conf. Opt. Commun.*, 2016, Paper W.2.B.1.
[32] K. Kawasaki, T. Sugimori, K. Watanabe, T. Saito, and R. Sugizaki, "Four-fiber fan-out for MCF with square lattice structure," in *Proc. Opt. Fiber Commun. Conf. Exhib.*, 2017, Paper W3H.4.
[33] P. Poggiolini, "The GN model of non-linear propagation in uncompensated coherent optical systems," *J. Lightw. Technol.*, vol. 30, no. 24, pp. 3852–3879, Dec. 2012.
[34] P. Poggiolini, G. Bosco, and A. Carena, "The LOGON strategy for low-complexity control plane implementation in new-generation flexible networks," in *Proc. Opt. Fiber Commun. Conf. Exhib.*, 2013, Paper OW1H.3.

Masahiko Jinno (Fellow, IEEE, Member, OSA) received the B.E. degree and M.E. degree in electronics engineering from Kanazawa University, Ishikawa, Japan, in 1984 and 1986, respectively, and the Ph.D. degree in engineering from Osaka University, Osaka, Japan, in 1995 for his work on ultra-fast optical signal processing based on nonlinear effects in optical fibers. He currently serves as a Professor of the Faculty of Engineering and Design with Kagawa University, Takamatsu, Japan. Prior to joining Kagawa University in October 2012, he was a Senior Research Engineer and Supervisor with Nippon Telegraph and Telephone (NTT) Network Innovation Laboratories, NTT Corporation conducting pioneering research on spectrum- and energy-efficient elastic optical networks (EONs). From 1993 to 1994, he was a Guest Scientist with the National Institute of Standards and Technology, Boulder, CO, USA. He authored or co-authored more than 180 peer-reviewed journal and conference papers in the fields of ultra-fast optical signal processing for high-capacity optical time division multiplexed transmission systems, optical sampling and optical time-domain reflectometry, ultra-wideband DWDM transmission systems in the L-band and S-band, ROADM systems, GMPLS and application-aware optical networking, EONs, and SDM networks. His current research interests include architecture, design, management, and control of optical networks, optical transmission systems, optical cross-connects, optical switches, and rate- and format-flexible optical transponders. He is a Fellow of the Institute of Electronics, Information and Communication Engineers (IEICE) and a Member of the Optical Society of America. He received the Young Engineer's Award in 1993, the Best Tutorial Paper Award in 2011, the Best Paper Award in 2012, the Achievement Award in 2017, and the Milestone Certificate in 2017 from the IEICE, the Best Paper Awards from the 1997, 1998, 2007, and 2019 Optoelectronics and Communications Conferences, the Best Paper Award from the 2010 ITU-T Kaleidoscope Academic Conference, and the Outstanding Paper Award in 2013 from the IEEE Communications Society Asia-Pacific Board.

Takahiro Kodama (Member, IEEE) received the B.E. degree from Ritsumeikan University, Shiga, Japan, in 2008 and the M.E. and Dr. Eng. degrees from Osaka University, Osaka, Japan, in 2010 and 2012, respectively. In 2012, he was selected as a Research Fellow of the Japan Society for the Promotion of Science. In 2014, he joined Mitsubishi Electric Corporation, Kanagawa, Japan. In 2016, he was a Research Assistant Professor with the Graduate Faculty of Interdisciplinary Research, University of Yamanashi, Yamanashi, Japan and was selected as an excellent young Researcher by the Ministry of Education, Culture, Sports, Science and Technology of Japan. Since 2019, he has been a Lecturer in the Faculty of Engineering and Design, Kagawa University. He has authored more than 50 papers in refereed journals and international conference papers. His research interests are in the area of optical access, metro and core networks, optical packet switching networks, digital signal processing, and optical signal processing. Dr. Kodama is a member of the IEEE and the Institute of Electronics, Information and Communication Engineers (IEICE) of Japan. He was the recipient of the 2011 IEEE Kansai Section Student Paper Award from the IEEE.

Tsubasa Ishikawa was born in Tokushima, Japan, in 1998. He is currently working toward the undergraduate degree with Kagawa University, Takamatsu, Japan.